Molecular and Morphological Characterization of Bis Benzimidazo Perylene Films and Surface-Enhanced Phenomena

ARTICLE *in* THE JOURNAL OF PHYSICAL CHEMISTRY B · MAY 2008

Impact Factor: 3.3 · DOI: 10.1021/jp077588h · Source: PubMed

4 AUTHORS:

Diogo Volpati
Mid Sweden University
24 PUBLICATIONS **187** CITATIONS
SEE PROFILE

Aldo E. Job
São Paulo State University
103 PUBLICATIONS **904** CITATIONS
SEE PROFILE

Ricardo F Aroca
University of Windsor
312 PUBLICATIONS **6,802** CITATIONS
SEE PROFILE

Carlos Constantino
São Paulo State University
159 PUBLICATIONS **2,128** CITATIONS
SEE PROFILE

Molecular and Morphological Characterization of Bis Benzimidazo Perylene Films and Surface-Enhanced Phenomena

D. Volpati,[†] A. E. Job,[†,‡] R. F. Aroca,[‡] and C. J. L. Constantino*[,†]

DFQB, Faculdade de Ciências e Tecnologia, UNESP, Presidente Prudente/SP, 19060-900, Brazil, and Materials and Surface Science Group, University of Windsor, Windsor/On, N9B3P4, Canada

Received: September 20, 2007; In Final Form: January 15, 2008

Thin solid films of bis benzimidazo perylene (AzoPTCD) were fabricated using physical vapor deposition (PVD) technique. Thermal stability and integrity of the AzoPTCD PVD films during the fabrication (∼400 °C at 10^{-6} Torr) were monitored by Raman scattering. Complementary thermogravimetric results showed that thermal degradation of AzoPTCD occurs at 675 °C. The growth of the PVD films was established through UV−vis absorption spectroscopy, and the surface morphology was surveyed by atomic force microscopy (AFM) as a function of the mass thickness. The AzoPTCD molecular organization in these PVD films was determined using the selection rules of infrared absorption spectroscopy (transmission and reflection−absorption modes). Despite the molecular packing, X-ray diffraction revealed that the PVD films are amorphous. Theoretical calculations (density functional theory, B3LYP) were used to assign the vibrational modes in the infrared and Raman spectra. Metallic nanostructures, able to sustain localized surface plasmons (LSP) were used to achieve surface-enhanced resonance Raman scattering (SERRS) and surface-enhanced fluorescence (SEF).

Introduction

The perylene derivatives shaped by π-conjugated systems form a class of materials used in different electronic devices owed to their low weight, easy and low cost of processing in comparison to the conventional semiconductors materials, and their interesting electrical and optical properties. For instance, it has been shown that thin films of these materials can be successfully used in optoelectronic and electronic devices such as solar cells, field effect transistors (FET), and light emitting diodes (LED).[1−3] These organic semiconductor molecules are the object of basic studies involving the growth of the thin films, their structure at molecular level, and their physical and chemical properties.[4,5] In this field of organic semiconductors, the perylene derivatives have received attention because of their high chemical and thermal stability and electro- and photoactivity.[6−8] Recently, studies involving the structural characterization of perylene derivatives and their application as transducer materials in sensing units have been reported[9,10] and also their nonlinear optical properties.[11,12] In addition, mobility "hole−electron-transport" can be reached in perylene derivatives by changing the lateral groups attached to the perylene chromophore.[13,14]

The application of these semiconductor organic materials in electronic devices is made in the form of thin films where the molecular organization plays an important role and mediates the electrical (and electronic device performance) and optical properties of these thin films. Therefore, basic characterization is required with Raman scattering and infrared absorption as tools that can help to understand physical−chemistry properties and the structural−morphological relationships.[15,16] Theoretical calculations involving the vibrational modes of these molecules are found to be an important guide in the assignments of the FTIR and Raman bands, which is a fundamental step to determine the molecular organization in the thin films.[17,18] In this work, thin films of a perylene derivative, bis benzimidazo perylene (AzoPTCD), were produced using the physical vapor deposition (PVD) technique, focusing on their morphological and molecular organization. PVD films were growth with different thicknesses onto different substrates and characterized through UV−vis absorption spectroscopy, atomic force microscopy (AFM), Raman scattering and FTIR complemented by theoretical calculations (DFT/B3LYP-6-311G(d,p)), X-ray diffraction, surface-enhanced resonance Raman scattering (SERRS), and surface-enhanced fluorescence (SEF). Langmuir−Blodgett (LB) films of AzoPTCD were also fabricated as references for the spectral analysis.

Experimental Methods

The sample of AzoPTCD whose molecular structure is given in Figure 1 was provided by Dr. J. Duff from Xerox Resource Centre of Canada. PVD films were deposited by vacuum evaporation (at 10^{-6} Torr and deposition rate of ca. 0.2 nm/s) with different mass thicknesses (10, 20, 30, 40, and 50 nm) monitored by a quartz crystal balance. PVD films of a given thickness were deposited simultaneously onto different substrates such as Ag island films (6 nm mass thickness), Au mirror, ZnSe, and quartz plates kept at room temperature (22 °C) depending on the characterization technique to be used. The thermal stability of the AzoPTCD was verified by comparing the Raman spectra of the PVD films with that of the powder. Thermogravimetric analysis (TG) carried out in a Netzsch equipment model 204 revealed that the AzoPTCD thermal degradation starts above 550 °C reaching a maximum at 675 °C (the evaporation to produce PVD films happens at ca. 400 °C).

Langmuir monolayers of AzoPTCD were transferred onto glass slides coated with 6 nm Ag island films using a KSV

* Corresponding author. E-mail: case@fct.unesp.br.
[†] UNESP.
[‡] University of Windsor.

10.1021/jp077588h CCC: $40.75
Published on Web 03/12/2008

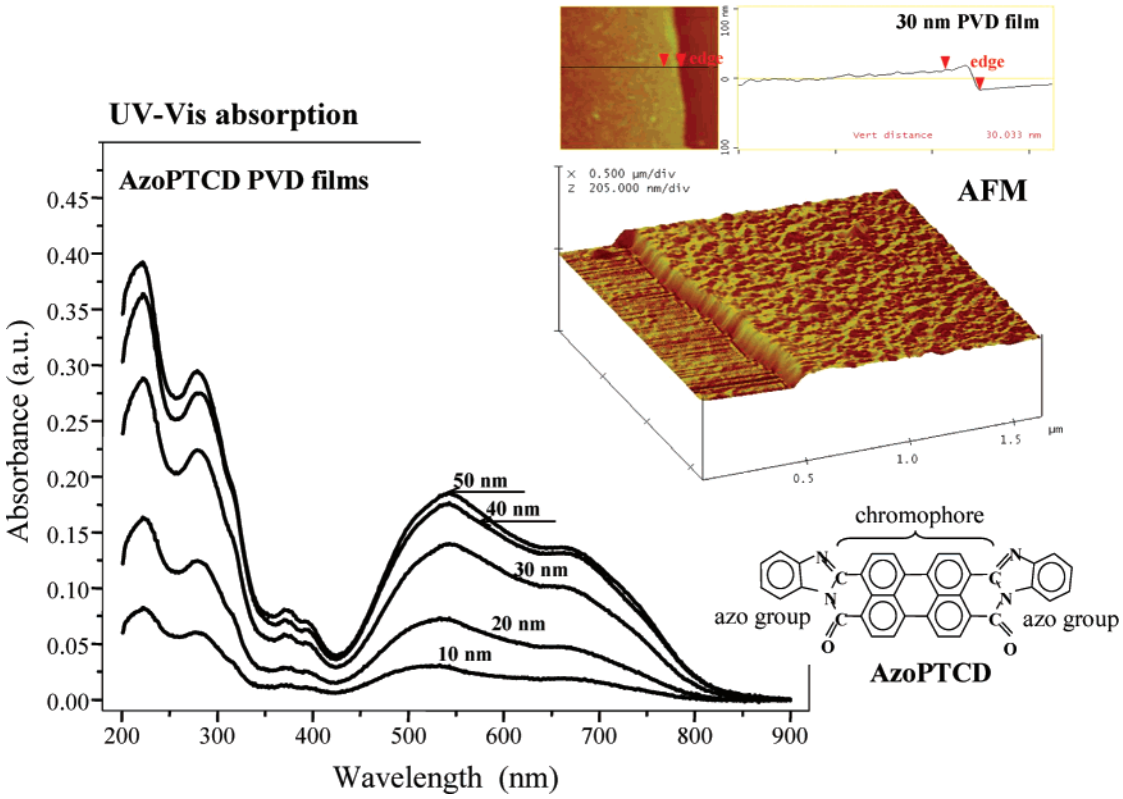

Figure 1. UV−Vis absorption spectra for PVD films with 10, 20, 30, 40, and 50 nm. Inset: AFM image for 30 nm PVD film and its profile along an edge made at the center of the film and the PTCD molecular structure.

Langmuir trough model 2000 to produce LB films. The subphase was ultrapure water (18.2 MΩ·cm) kept at 22 °C. Solutions of AzoPTCD were prepared with 10% trifluoroacetic acid (TFA) in dichloromethane, and the LB films were fabricated using a Z-type deposition. Monomolecular LB films were built keeping a constant surface pressure at 28 mN/m, which corresponds to the condensed phase in the Langmuir surface pressure vs molecular area isotherm.

UV−vis and surface plasmon spectra were recorded with a spectrophotometer Varian model Cary 50. The AzoPTCD powder was dispersed in KBr powder to produce pellets that were used in transmission FTIR spectroscopy. Transmission and reflection−absorption infrared spectra were recorded at the mid-infrared region using a Bruker spectrometer model Vector 22 equipped with a DTGS detector, 4 cm^{-1} spectral resolution, and 128 scans. The reflection−absorption spectra of 40 nm PVD films were recorded at an incident angle of 80° using an A118 Bruker accessory, which uses Au mirrors. AFM images were collected using a Digital Instrument model Nanoscope IV with a tip of silicon nitride and a spring constant of 0.12 N/m. X-ray diffraction was conducted for both powder and PVD films (40 and 160 nm) using a Rigaku diffractometer.

Resonance Raman scattering (RRS), SERRS, and SEF were obtained with a Renishaw in-Via Raman microscope equipped with a computer-controlled three-axis-encoded (XYZ) motorized stage with a minimum step of 0.1 μm. The in-Via uses a Leica microscope, and the high throughput of the instrument permits the use of very low powered lasers. Typically, the power of 514.5 and 785 nm laser lines at the sample were in the 1−100 μW range. The spectrograph is equipped with 1800 and 1200 grooves/mm gratings with additional notch filters. Raman spectra were recorded at room temperature (22 °C) with ca. 4 cm^{-1} resolution while fluorescence spectra were recorded at different temperatures (from −150 to +250 °C) using a Linkan 600 temperature stage. Data acquisition and analysis were carried out using WiRE software for windows and Galactic Industries GRAMS/32 C software.

Results and Discution

Growth of AzoPTCD PVD Films. UV−vis and AFM. The growth of PVD films with 10, 20, 30, 40, and 50 nm mass thicknesses deposited onto quartz substrates were monitored using UV−vis absorption spectroscopy as shown in Figure 1. The inset in Figure 1 presents an AFM image for a 30 nm PVD film to show its profile along an edge revealing that the 30 nm mass thickness measured by the crystal quartz oscillator in the evaporator machine is in good agreement with the real thickness of the PVD film measured by AFM. Similar results were found for PVD films with 10, 20, and 40 nm mass thicknesses. Plots of the film's absorbance at 540 nm as a function of the thickness shown in Figure 2a corroborate the results obtained in AFM. The absorbance increases linearly up to 40 nm, indicating that a proportional amount of material has been deposited onto the substrates up to this thickness. An odd result was obtained for the 50 nm PVD film. However, thicker PVD films can be produced by evaporating AzoPTCD in several steps. For instance, a 160 nm PVD film can be fabricated built in four steps of 40 nm each as shown in Figure 2b. Figure 2c presents the optical images obtained using both a digital camera and a microscope with a 50× objective lens for 160 nm PVD film, revealing a smooth morphology of the surface at micrometer scale. The morphology of a 160 nm mass thickness PVD film at nanometer scale can be seen in the AFM image in Figure 2c, where the edge is also shown.

The absorption spectra of perylene tetracarboxylic derivatives containing one or two perylene chromophores usually consist of one electronic transition with a characteristic vibronic structure.[19,20] Figure 3 shows the UV−vis absorption spectrum for AzoPTCD solution with the characteristic vibronic structure

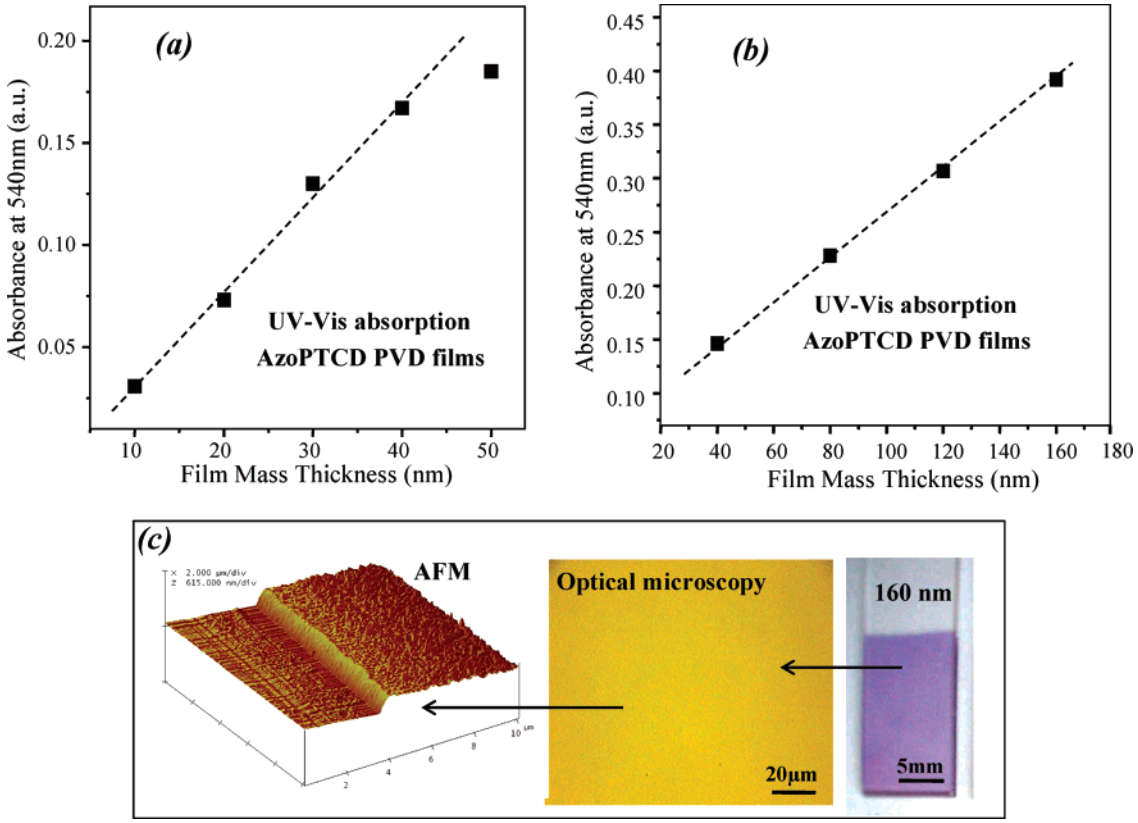

Figure 2. (a) Absorbance at 540 nm vs mass thickness for PVD films with 10, 20, 30, 40, and 50 nm; (b) absorbance at 540 nm vs mass thickness for PVD films with 40, 80, 120, and 160 nm; (c) optical images collected using the digital camera, the optical microscope (50× objective lens) and an AFM image for 160 nm PVD film.

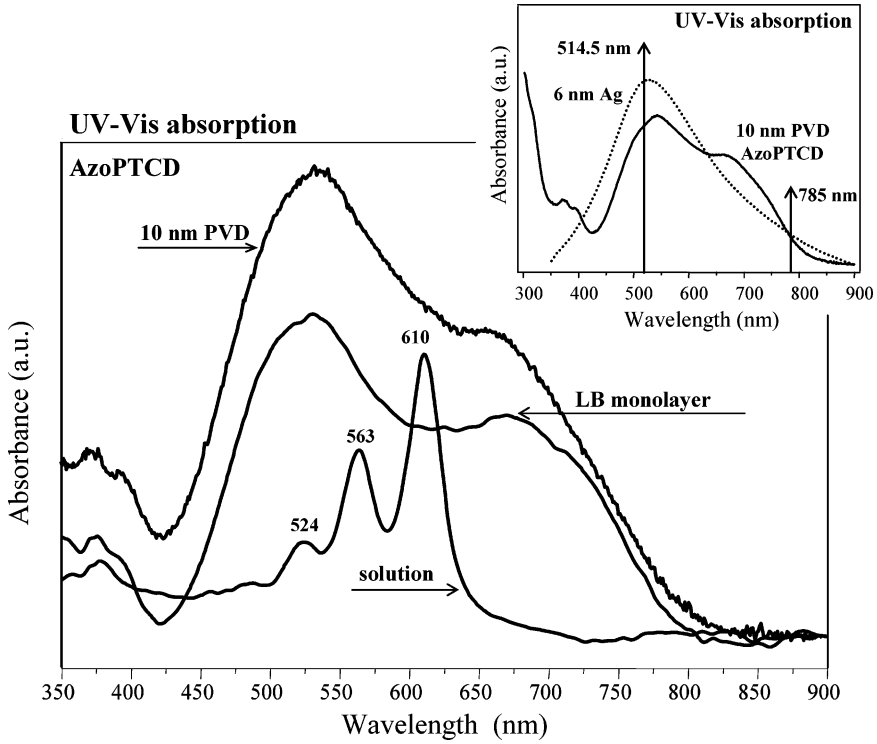

Figure 3. UV−Vis absorption spectra of AzoPTCD for solution, LB monolayer on glass and 10 nm PVD film on quartz. All curves were normalized to fit at the same Y axis. The inset shows the laser lines at 514.5 and 785 nm in full-resonance and in preresonance, respectively, with the electronic absorption for both AzoPTCD film and 6 nm Ag islands.

associated with $\pi-\pi^*$ transition of the perylene chromophore with a 0−0 band at 610 nm, followed by subsequent vibronic transitions at 563 nm and at 524 nm. The UV−vis absorption spectra for the LB monolayer deposited onto glass and the 10 nm PVD film onto quartz are also given in Figure 3. An intense blue-shift component with a broad maximum at 540 nm and a red-shift component at 670 nm are observed for both PVD films and the LB monolayer. Kasha's point-dipole model provides a

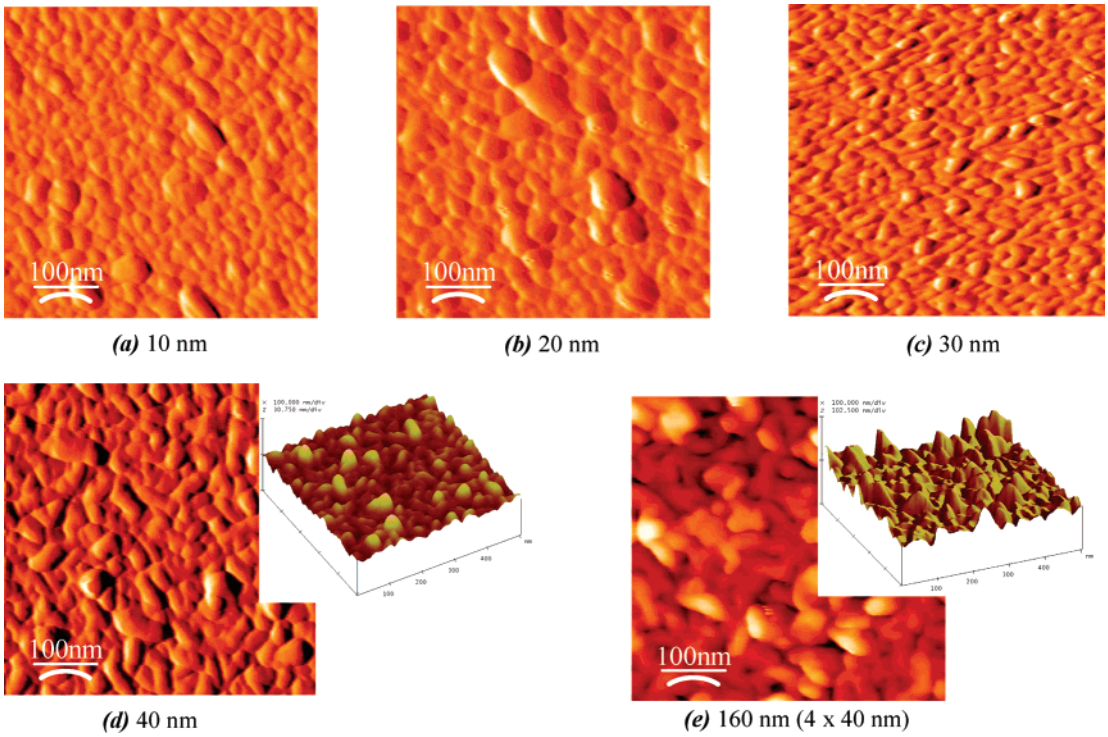

(a) 10 nm *(b)* 20 nm *(c)* 30 nm

(d) 40 nm *(e)* 160 nm (4 x 40 nm)

Figure 4. AFM images recorded using the tapping mode for AzoPTCD PVD films with different thicknesses: (a) 10 nm; (b) 20 nm; (c) 30 nm; (d) 40 nm; (e) 160 nm (4 × 40 nm). In the case of 40 and 160 nm, the 3D AFM images are also shown.

TABLE 1: Average Roughness, Aggregate Diameter, and Aggregate Height for the AzoPTCD PVD Films with Different Thicknesses

			particle size (nm)					
			small		medium		large	
sample, nm	area (μm^2)	rms (nm)	diameter	height	diameter	height	diameter	height
10	11 × 11	1.60	19.70	0.88	28.15	1.87	50.67	6.94
	1 × 1	1.43						
	0.55 × 0.55	0.846						
20	11 × 11	2.32	26.50	1.87	43.35	3.20	69.86	13.09
	1 × 1	1.55						
	0.55 × 0.55	1.65						
30	11 × 11	1.83	13.21	1.18	17.92	4.84	35.84	8.95
	1 × 1	1.37						
	0.55 × 0.55	1.22						
40	11 × 11	2.32	17.28	1.24	37.54	7.54	59.62	9.14
	1 × 1	1.67						
	0.55 × 0.55	2.58						
160	11 × 11	12.69	62.5	9.42	97.65	22.28	132.81	57.99
	1 × 1	10.93						
	0.55 × 0.55	8.74						

rationale for the observed band splitting.[21] The extreme cases are represented by a "head-to-tail" arrangement of the dipoles (J-aggregates), which leads to a red-shifted band. A blue-shifted band arises from an unfavorable "card pack" arrangement of the dipoles (H-aggregates). The strong red- and blue-shift band components observed in the UV−vis absorption spectra of the films is an indication of an intermediate case of J and H aggregates for the LB monolayer with the molecules tilted on the substrate (as in the Langmuir films, result not shown) while for the PVD the molecules are on top of each other, forming a multilayer with the H and J aggregates. Both cases result in the apparent band splitting, which has been observed for other perylene derivatives.[18,22−24] In the inset of Figure 3 it is also shown that the 514.5 laser line is in full-resonance, while the 785 nm line is in preresonance, with the electronic absorption of AzoPTCD and the surface plasmon of Ag nanostructures. The latter is a necessary condition to activate the enhancement mechanisms in Ag islands to observe surface-enhanced phenomena.[25,26]

Surface Morphology of AzoPTCD PVDF Films. AFM. The AzoPTCD PVD film's morphology was probed by AFM using the tapping mode. Figure 4 (a, b, c, and d) shows the topographic images (500 × 500 nm) for PVD films with 10, 20, 30, and 40 nm. The Figure 4e refers to the 160 nm PVD film prepared in four steps of 40 nm each. AFM images were also obtained in areas of 11 × 11 μm and 1 × 1 μm (figures not shown). Topographically on a nanometer scale, the images show domains at the surface attributed to the formation of aggregates during the evaporation of the AzoPTCD powder to produce the PVD films. The roughness and the dimensions of the domains were measured using the software of the Nanoscope IV instrument and are given in Table 1. It was observed that the average

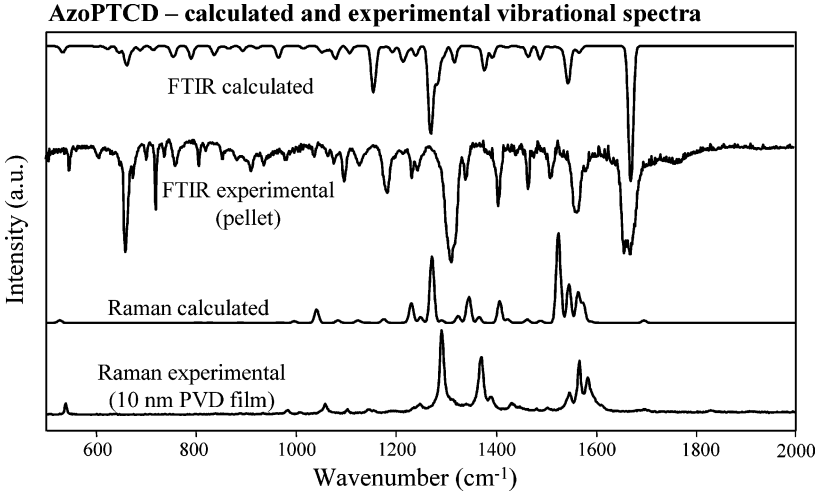

Figure 5. Experimental and calculated (DFT/6-311G basis set) infrared and Raman spectra.

TABLE 2: Wavenumbers and Relative Intensities of the Calculated and Experimental Infrared Bands for AzoPTCD in KBr Pellet (Figure 5)

calculated		FTIR experimental		
wavenumber (cm^{-1})	relative intensity	wavenumber (cm^{-1})	relative intensity	assignments[a]
630	4	645	25	torsion (perylene)
712	2	696	16	torsion (perylene)
750	15	748	82	C−H wagging (azo)
775	3	760	57	C−H wagging (perylene)
838	8	806	17	breathing (chromophore)
871	9	842	22	C−H wagging (chromophore)
914	7	885	22	breathing (azo)
1035	9	985	26	C−H bending in-plane (azo)
1142	10	1157	39	C−H bending in-plane (perylene)
1166	5	1184	21	C−H bending in-plane (perylene)
1212	34	1236	42	C−H bending in-plane (chromophore)
1267	12	1282	30	C−H bending in-plane (chromophore)
1291	7	1297	25	C−H bending + ring stretching (perylene)
1320	69	1356	100	C−H bending + ring stretching (perylene)
1336	29	1366	45	C−N stretching + ring stretching + C−H bending (perylene)
1364	12	1385	32	C−N stretching + ring stretching + C−H bending (perylene)
1420	8	1446	49	C−H bending +ring stretching (chromophore)
1520	18	1501	52	ring stretching + C−H bending (azo)
1525	10	1543	31	ring stretching + C−H bending (azo)
1577	27	1590	45	C═N stretching + ring stretching
1598	5	1607	57	ring stretching (chromophore)
1693	100	1682	86	C═O symmetric stretching
1696	99	1693	87	C═O antisymmetric stretching

[a] The term perylene refers to vibrational modes present in the whole molecule, the term chromophore refers to vibrational modes present in the moiety, and the term azo refers to vibrational modes present in the lateral group (see Figure 7). The terms in-plane and out-of-plane refer to the plane that contains the chromophore.

roughness is around 10% of the thickness for the PVD films with 10 and 20 nm and it is around 5% for the PVD films with 30, 40, and 160 nm, which is at the range found for pentacene PVD thin films.[27] The roughness found to be between 5 and 15% of the thickness for the AzoPTCD domains in the PVD films was classified as small, medium, and large, considering diameter and height. A relationship of both aggregate diameter and aggregate height to thickness was not found for the AzoPTCD PVD films between 10 and 40 nm (only the height of medium aggregates follows the thickness). Domains were found larger and higher for the 160 nm PVD film as a probable consequence of the superposition of the "4 layers" of 40 nm each. All the parameters (surface roughness, aggregate diameter, and aggregate roughness) are on the nanometer scale, which is consistent with the smooth surface observed on a micrometer scale through optical microscopy (Figure 2c).

Molecular Organization of AzoPTCD in PVD Films. FTIR. The molecular organization study of the AzoPTCD in PVD films was preceded by an investigation of the fundamental normal modes of the AzoPTCD (infrared absorption and Raman scattering) through theoretical calculations using DFT/6-311G basis set. The infrared and Raman spectra of the AzoPTCD are given in Figure 5. Notably, a relative good agreement was obtained between the calculated and the experimental spectra for AzoPTCD. Tables 2 and 3 contain the wavenumbers and relative intensities for both experimental and calculated vibrational infrared and Raman bands, respectively, based on the calculation and the literature.[28,29]

The molecular organization of the AzoPTCD in PVD films was investigated by comparing the transmission FTIR spectrum of the film onto ZnSe and the reflection−absorption FTIR spectrum of the film onto the Au mirror. The transmission FTIR

TABLE 3: Wavenumbers and Relative Intensities of the Calculated and Experimental Raman Bands for AzoPTCD in 10 nm PVD Film (Figure 5)

Raman calculated		Raman experimental		
wavenumber (cm^{-1})	relative intensity	wavenumber (cm^{-1})	relative intensity	assignments[a]
526	3	539	18	breathing (chromophore)
1039	15	1052	10	C−H bending in-plane (azo)
1229	22	1240	9	C−H bending (chromophore)
1269	73	1290	100	C−H bending + ring stretching (chromophore)
1324	6	1360	74	C−N stretching + ring stretching + C−H bending (perylene)
1345	29	1371	18	C−H bending in-plane + ring stretching (chromophore)
1525	100	1547	29	C═N stretching + ring stretching (perylene)
1545	42	1567	66	ring stretching (chromophore)
1563	34	1583	42	C═C stretching (perylene)

[a] The term perylene refers to vibrational modes present in the whole molecule, the term chromophore refers to vibrational modes present in the moiety, and the term azo refers to vibrational modes present in the lateral group (see Figure 7). The terms in-plane and out-of-plane refer to the plane that contains the chromophore.

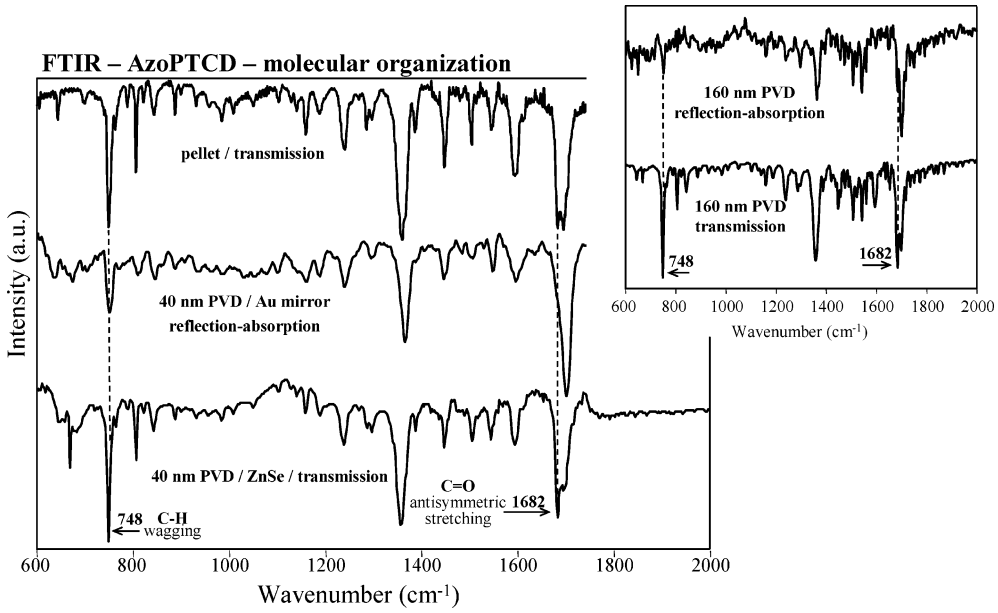

Figure 6. FTIR transmission spectra for AzoPTCD powder in a KBr pellet and the 40 nm PVD film on ZnSe and the reflection−absorption spectrum for a 40 nm PVD film on a Au mirror. The inset shows the FTIR transmission and reflection−absorption spectra for a 160 nm PVD film.

spectrum of the AzoPTCD powder in a KBr pellet is taken as reference. These three FTIR spectra are presented in Figure 6. The differences in the relative intensities for the PVD film spectra (transmission and reflection−absorption modes) suggest a strong anisotropy in these films in terms of molecular organization.

Molecular organization was extracted from the FTIR spectroscopic data (transmission and reflection−absorption modes) by applying the surface selection rules,[30−32] which can be briefly explained as follows. The incident electric field of the infrared radiation is parallel to the substrate surface in the transmission mode while in the reflection−absorption mode the electric field is polarized perpendicular to the substrate surface, considering the metal used (Au) and the incident angle (80°), which is illustrated in Figures 7a and 7b, respectively. The infrared absorption by a fixed molecule in space depends on the interaction between the electric field of the incident radiation ($\vec{E}$) and the dipole derivative of each normal mode ($\vec{\mu}'$). The intensity (I) of this absorption is given by the scalar product $I = \vec{E}\vec{\mu}'$. Therefore, once the direction of the electric field of the incident radiation is known in transmission and reflection−absorption modes, the molecular organization can be determined using certain FTIR bands whose μ' components are well established.[18] For instance, the μ' component of the FTIR absorption band at 748 cm^{-1} assigned to C−H wagging (ref 22 and calculation) is shown in Figure 7c. Since its relative intensity is stronger in the transmission mode than in the reflection−absorption (Figure 6), it can be concluded that the AzoPTCD is placed preferentially with its chromophore plane perpendicular to the substrate surface. Besides, the absorption band at 1682 cm^{-1} assigned to C═O antisymmetric stretching (ref 18 and calculation), whose μ' component is shown in Figure 7d, has a relative intensity much stronger in the transmission mode than in the reflection−absorption where it is just a shoulder (Figure 6). This not only confirms that the AzoPTCD is placed preferentially perpendicular to the substrate but also that the molecule is supported by its longer axis as illustrated in Figure 7e. The same results were found for 160 nm PVD film, revealing that the molecular organization is kept during each step of the PVD film fabrication (inset in Figure 6). This approach has been used by our group to determine the molecular organization in thin films for different classes of materials including not only small molecules such as phthalocyanines,[33] nitrochrysenes,[34] or even other perylene derivatives[35] but also macromolecules such as lignins from sugar cane,[36,37] ruthenium biphosphine complex,[38] or luminescent polymers.[39] It should be mentioned that the molecular organization is not only governed by attractive and repulsive forces among the molecules related to their chemical structures. Experimental factors such as rate deposition, substrate temperature, and vacuum level may be tuned to induce

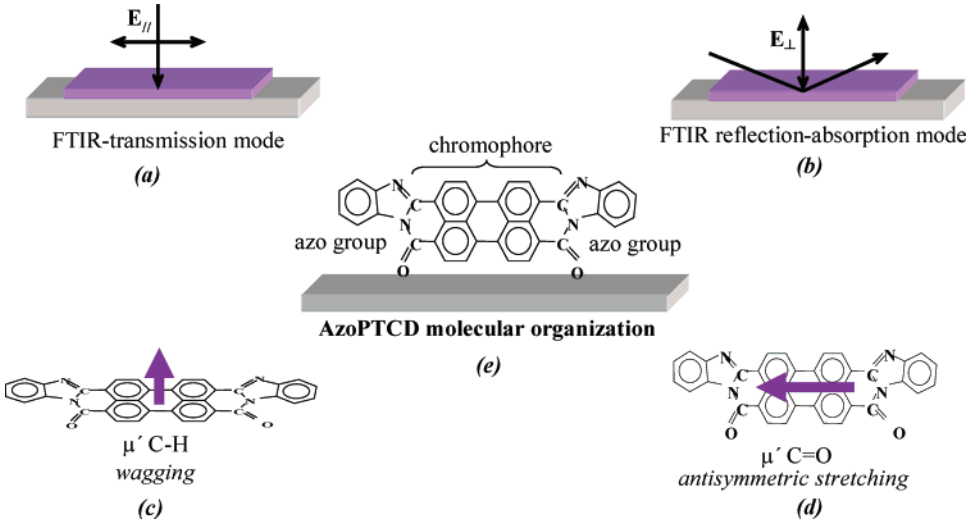

Figure 7. (a) Transmission mode: electric field (E) of light parallel to the substrate surface; (b) reflection−absorption mode: incident angle of light at 80° maximizing the component of the electric field (E) perpendicularly to the substrate surface; (c) component μ' of C−H wagging (out-of-plane); (d) component μ' of C═O antisymmetric stretching (in-plane); (e) molecular organization found for the AzoPTCD in the PVD films.

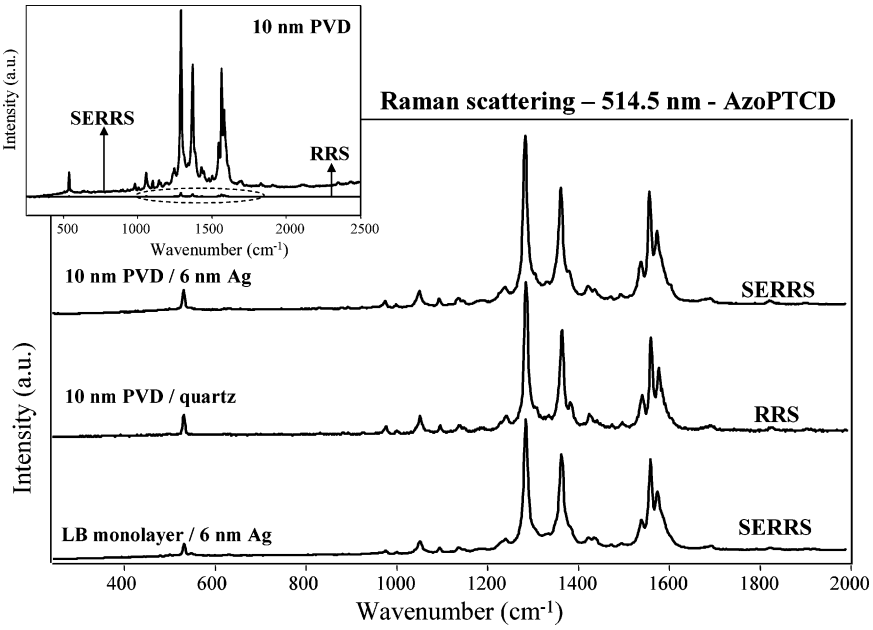

Figure 8. SERRS and RRS spectra for 10 nm PVD film and SERRS spectrum for LB monolayer of the AzoPTCD. The inset shows the SERRS and RRS spectra of the AzoPTCD 10 nm PVD film at the same scale.

different molecular organizations. The crystallinity of the PVD film was investigated using X-ray diffraction (XRD). Diffractograms were recorded for AzoPTCD powder and the 40 nm PVD film. The results revealed that the powder is crystalline but the PVD film is amorphous (figure not shown). A 400 nm PVD film was then produced through 10 steps of 40 nm each to check if the result could be related to the small thickness of the PVD film. The results showed that the 400 nm PVD film is also amorphous.

Surface-Enhanced Resonance Raman Scattering (SERRS). The RRS (514.5 nm excitation) contains a small number of characteristic molecular wavenumbers listed in Table 3. The SERRS and RRS spectra recorded for the 10 nm PVD film and the LB monolayer of the AzoPTCD are shown in Figure 8. The enhancement factor can be estimated simply by the ratio SERRS/RRS for the signal intensities and considering the different laser powers at the sample since only a very low RRS signal could be seen even using high laser power. It was found an enhancement factor of ca. 450 for the 10 nm PVD film and ca. 500 for the LB monolayer. If it is considered that the intensification of the RRS in relation to the conventional Raman scattering is about that of the extinction coefficient, which is ca. 10^4 for the PTCD family where AzoPTCD belongs,[18] the SERRS signal in relation to the Raman scattering is amplified about 10^6-10^7, which is expected on the average.[26,40] Besides, a close comparison of the wavenumbers for both RRS and SERRS spectra indicates that the AzoPTCD is physically adsorbed onto the Ag surface when forming the PVD films, which was observed previously for LB films as well.[41] Therefore, since there is no chemical interaction between the AzoPTCD and the Ag nanostructures, the surface-enhancement must be related to the so-called electromagnetic mechanism, whose origin is assigned to the amplification of the electromagnetic field around the metallic nanoparticles (Ag islands in this case). This topic is discussed in detail elsewhere.[26,40]

The fact that the intensification of the RRS in relation to the conventional Raman scattering is about that of the extinction coefficient ($\sim 10^4$) for the AzoPTCD might explain why the RRS

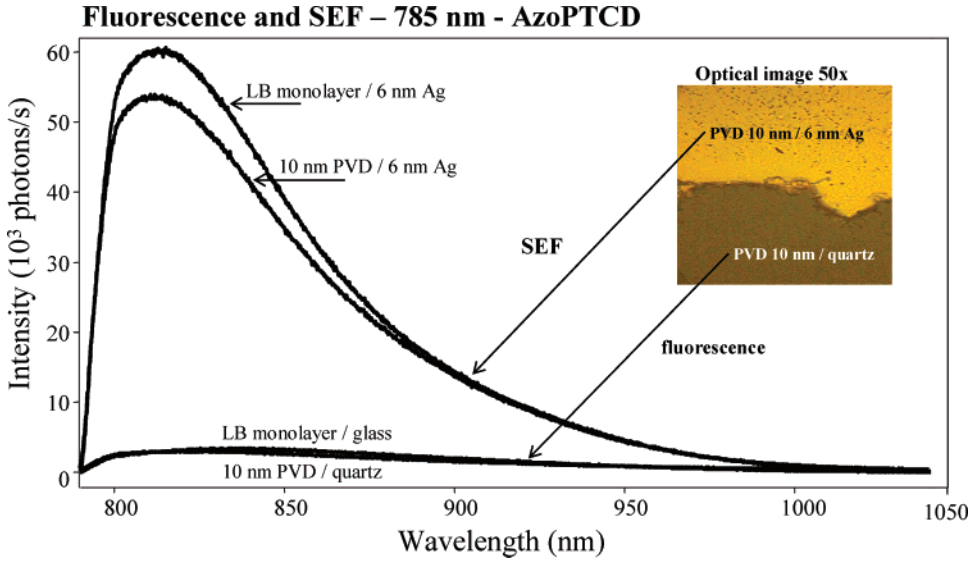

Figure 9. Fluorescence spectra for a 10 nm PVD film on quartz and an LB monolayer on glass and SEF spectra for both films on Ag islands. The optical image refers to a 10 nm PVD film on glass and Ag islands.

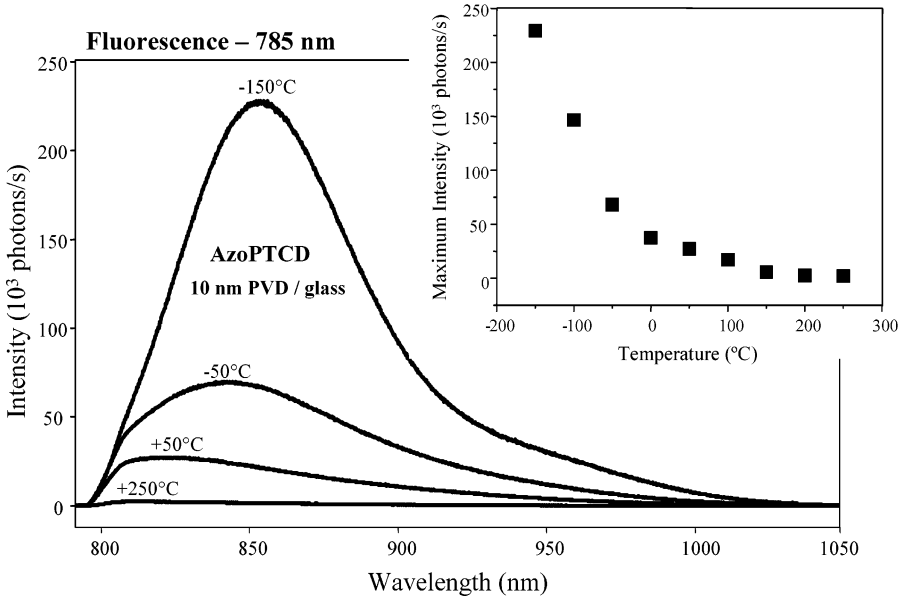

Figure 10. Fluorescence spectra for 10 nm PVD film on quartz recorded at different temperatures.

is observed for the 514.5 nm laser line, which is in full-resonance with the electronic absorption of the PVD film, and the excimer fluorescence is observed for the 785 nm, which is in preresonance with the electronic absorption of the PVD film as shown in the inset in Figure 3. Finally, the similarity between SERRS spectra for both PVD films and LB monolayer is other evidence that the AzoPTCD is not thermally degraded during the fabrication of the PVD films.

Surface-Enhanced Fluorescence (SEF). The electronic characterization of the AzoPTCD was carried out through emission (fluorescence and SEF) in addition to the UV−vis absorption. Figure 9 shows the fluorescence for a 10 nm PVD film onto quartz and LB monolayer onto glass and SEF for both of these films when deposited onto the 6 nm Ag islands excited at 785 nm. The enhancement factor was estimated by direct comparison of the maximum emission at 813 nm (at 23 °C), considering the signal ratio of the film onto Ag islands and onto quartz or glass. The ratio SEF/fluorescence was found to be ca. 40 for the 10 nm PVD film and 50 for the LB monolayer, which is within the range, considering what we have found for other perylene derivatives. For instance, it was found to be 10 for thio bis (benzimidazo) perylene,[24] 400 for bis (phenethylimido) perylene,[22] 6 for a luminescent polymer,[39] and 99 for a polymer containing an azo dye.[42] It is known that the energy quenching for molecules directly adsorbed on the metal surface normally diminishes the fluorescence signal. In fact, fluorescence enhancement is observed to increase with the separation from the metal surface to reach a maximum at an optimum distance where SEF enhancement overpowers quenching.[23,43,44] Therefore, the SEF observed here is in agreement with the molecular organization found through FTIR data revealing that the PTCD chromophore is not touching the surface in a flat-on fashion.

The excimer fluorescence was recorded at different temperatures as well. Figure 10 presents the spectra of the AzoPTCD 10 nm PVD film at +250, +50, −50 and −150 °C. These spectra belong to a series of spectra recorded as following: +22 °C → 0 °C → −50 °C → −100 °C → −150 °C → −100 °C→ −50 °C → 0 °C → +50 °C → +100 °C → +150 °C → +200 °C → +250 °C → +200 °C → +150 °C → +100 °C → +50 °C → +22 °C. The inset in Figure 10 shows how the

maximum intensity decreases as the temperature increases. Since the emission for PTCD derivatives is attributed to excimer formation,[45] the observation of a high emission for the AzoPTCD studied here is related to the formation of organized structures or molecular stacking in the PVD (and LB monolayers), which requires the chromophore to be arranged in parallel and to overlap the ring systems (excimer formation ability). Therefore, the decrease of maximum intensity with temperature can be related to both the lack of molecular packing, which makes the excimer formation more difficult, and the phonon background interference as the temperature is increased.[24] However, the signal intensity is recovered when room temperature (+22 °C) is reached, which is an important feature, considering applications involving electrooptical devices. Finally, the shift of the maximum intensity to lower wavelength with temperature seen in Figure 10 can also be related to the loss of the film's molecular packing once a shorter "electron free way" is produced, and consequently higher energy is absorbed or emitted (lower wavelength).

Conclusion

Thin films of bis benzimidazo perylene (AzoPTCD) have been produced with different mass thicknesses using the physical vapor deposition (PVD) technique. The thermogravimetric analysis and the Raman scattering techniques ensure that the molecule is not degraded during the film fabrication process. The PVD film grows linearly up to 40 nm; however, thicker films can be produced simply by adding steps of 40 nm or less. The surface morphology was characterized at micrometer and nanometer scales through micro-Raman and atomic force microscopy (AFM), respectively. A very smooth and homogeneous surface on a micrometer scale presents a roughness between 5 and 10% on a nanometer scale in relation to the mass thickness of the films. The assignments of the infrared and Raman vibrational modes have been carried out based on DFT calculations. Considering both the FTIR results (transmission and reflection−absorption modes) and the surface selection rules, it was possible to determine that the AzoPTCD molecules are organized in the PVD films with the chromophore plane preferentially perpendicular to the substrate (edge-on orientation) held up by the longer molecular axis. Besides, X-ray diffraction showed that the organized PVD films are amorphous. Surface-enhanced resonance Raman scattering (SERRS) and surface-enhanced fluorescence (SEF) with enhancement factors around 10^6 and 50, respectively, have been found that are mainly attributed to the electromagnetic mechanism. Fluorescence as function of the temperature for AzoPTCD PVD films revealed that the signal is reversible at the investigated range (from −150 to +250 °C). Langmuir−Blodgett (LB) films were also produced and applied to the SERRS and SEF studies.

Acknowledgment. FAPESP and CNPq (CIAM and IMMP) from Brazil and NSERC from Canada for the financial support. Daniel J. Ross from University of Windsor for the theoretical calculations and Dr. Paulo N. L. Filho from FC/UNESP for the X-ray facilities. Dr. Aldo E. Job acknowledges CAPES for his fellowship.

References and Notes

(1) Zafer, C.; Kus, M.; Turkmen, G.; Dincalp, H.; Demic, S.; Kuban, B.; Teoman, Y.; Icli, S. *Sol. Energy Mater. Sol. Cells* **2007**, *91*, 427.

(2) Unni, K. N. N.; Pandey, A. K.; Alem, S.; Nunzi, J. M. *Chem. Phys. Lett.* **2006**, *421*, 554.

(3) Colle, M.; Tsutsui, T. *Synth. Met.* **2000**, *111*, 95.

(4) Gustafsson, J. B.; Moons, E.; Widstrand, S. M.; Johansson, L. S. O. *Surf. Sci.* **2006**, *600*, 4758.

(5) Berger, S.; Heimer, K.; Mack, H. G.; Ziegler, C. *Appl. Surf. Sci.* **2005**, *252*, 81.

(6) Aroca, R.; Del Cano, T.; DeSaja, J. A. *Chem. Mater.* **2003**, *15*, 38.

(7) Aroca, P.; Aroca, R. *Langmuir* **1990**, *6*, 1051.

(8) De SajaGonzalez, J.; Aroca, R.; Nagao, Y.; DeSaja, J. A. *Spectrochim. Acta, Part A* **1997**, *53*, 173.

(9) Heimer, K.; Wuesten, J.; Lach, S.; Ziegler, C. *J. Chem. Phys.* **2007**, *126*, 164709.

(10) Silva, B. A.; Antunes, P. A.; Pasquini, D.; Curvelo, A. A. S.; Aroca, R. F.; Riul, A., Jr.; Constantino, C. J. L. *J. Nanosci. Nanotechnol*. **2007**, *7* (2), 510.

(11) Boni, L.; Constantino, C. J. L.; Misoguti, L.; Aroca, R. F.; Zilio, S. C.; Mendonca, C. R. *Chem. Phys. Lett.* **2003**, *371* (5−6), 744.

(12) Oliveira, S. L.; Corrêa, D. S.; Misoguti, L.; Constantino, C. J. L.; Aroca, R. F.; Zilio, S. C.; Mendonça, C. R. *Adv. Mater.* **2005**, *17* (15), 1890

(13) Harowitz, G.; Kouki, F.; Spearman, P.; Fchou, D.; Nogues, C.; Pan, X.; Garnier, F. *Adv. Mater.* **1996**, *8*, 242.

(14) Méndez, H.; Thurzo, I.; Zahn, D. R. T. *Phys. Rev. B* **2007**, *75*, 045321.

(15) Kam, A. P.; Aroca, R.; Duff, J. *Chem. Mater*. **2001**, *13* (12), 4463.

(16) Del Cano, T.; Duff, T.; Aroca, R. *Appl. Spectrosc.* **2002**, *56*, 744.

(17) Ong, K. K.; Jensen, J. O.; Hameka, H. F. *J. Mol. Struct. (THEOCHEM)* **1999**, *459*, 131.

(18) Antunes, P. A.; Constantino, C. J. L.; Aroca, R.; Duff, J. *Appl. Spectrosc.* **2001**, *55* (10), 1341.

(19) Mercadante, R.; Trsic, M.; Duff, J.; Aroca, R. *J. Mol. Struct*. (*THEOCHEM*) **1997**, *394*, 215.

(20) Aroca, R. F.; Constantino, C. J. L. *Langmuir* **2000**, *16*, 5425.

(21) Ramamurthy, V. *Photochemistry in Organized and Constrained Media*; VCH Publishers: New York, 1991; Chapter 15.

(22) Aroca, R. F.; Constantino, C. J. L.; Duff, J. *Appl. Spectrosc*. **2000**, *54* (8), 1120.

(23) Antunes, P. A.; Constantino, C. J. L.; Aroca, R. F. *Langmuir* **2001**, *17*, 2958.

(24) Constantino, C. J. L.; Duff, J.; Aroca, R. *Spectrochim. Acta, Part A* **2001**, *57*, 1249.

(25) Moskovitz, M. *Rev. Mod. Phys*. **1985**, *57*, 783.

(26) Kneipp, K.; Moskovits, M.; Kneipp, H. *Surface-Enhanced Raman Scattering − Physics and Applications*; Springer-Verlag: Duesseldorf, Germany, 2006.

(27) Itoh, T.; Yamauchi, N. *Appl. Surf. Sci.* **2007**, *253*, 6196.

(28) Kam, A.; Aroca, R.; Duff, J.; Tripp, C. P. *Chem. Mater*. **1998**, *10*, 172.

(29) Rodriguez-Liorent, S.; Aroca, R.; Duff, J. *J. Mater Chem* **1998**, *8*, 629.

(30) Bradshaw, A. M.; Schweizer, E. *Spectroscopy of Surfaces*; John Wiley & Sons: Toronto, 1988.

(31) Born, M.; Wolf, E. *Principles of Optics*; Pergamon Press: Oxford, 1987.

(32) Debe, M. K. *Prog. Surf. Sci*. **1987**, *24*, 1.

(33) Del Canõ, T.; Parra, V.; Rodriguez-Mendez, M. L.; Aroca, R. F.; DeSaja, J. A. *Appl. Surf. Sci.* **2005**, *246* (4), 327.

(34) Carrasco-Flores, E. A.; Clavijo, R. E.; Campos-Vallette, M. M.; Aroca, R. F. *Spectrochim. Acta, Part A* **2005**, *61*, 509.

(35) Del Caño, T.; Parra, V.; Rodríguez-Méndez, M. L.; Aroca, R.; DeSaja, J. A. *Org. Electron.* **2004**, *5*, 107.

(36) Pasquini, D.; Balogh, D. T.; Antunes, P. A.; Constantino, C. J. L.; Curvelo, A. A. S.; Aroca, R. F.; Oliveira, O. N., Jr. *Langmuir* **2002**, *18*, 6593.

(37) Pereira, A. A.; Martins, G. F.; Antunes, P. A.; Conrrado, R.; Pasquini, D.; Job, A. E.; Curvelo, A. A. S.; Ferreira, M.; Riul, A., Jr.; Constantino, C. J. L. *Langmuir* **2007**, *23*, 6652.

(38) Wohnrath, K.; Constantino, C. J. L.; Antunes, P. A.; dos Santos, P. M.; Batista, A. A.; Aroca, R. F.; Oliveira, O. N., Jr. *J. Phys. Chem. B* **2005**, *109*, 4959.

(39) Ferreira, M.; Constantino, C. J. L.; Olivati, C. A.; Vega, M. L.; Balogh, D. T.; Aroca, R. F.; Faria, R. M.; Oliveira, O. N., Jr. *Langmuir* **2003**, *19*, 8835.

(40) Aroca, R. *Surface Enhanced Vibrational Spectroscopy*; Wiley: Canada, 2006.

(41) Constantino, C. J. L.; Aroca, R. F. *J. Raman Spectrosc.* **2000**, *31*, 887.

(42) Constantino, C. J. L.; Aroca, R. F.; Mendonça, C. R.; Mello, S. V.; Balogh, D. T.; Oliveira, O. N., Jr. *Spectrochim. Acta, Part A* **2001**, *57*, 281.

(43) Chance, R. R.; Prock, A.; Silbey, R. *Adv. Chem. Phys*. **1978**, *37*, 1.

(44) Kummerlen, J.; Leitner, A.; Brunner, H.; Aussenegg, F. R.; Wokaun, A. *Mol. Phys.* **1993**, *80*, 1031.

(45) Tanaka, J. *Bull. Chem. Jpn.* **1963**, *36*, 1237.